Directional image denoising method based on the relative intersection of confidence intervals rule

Damir Sersic [1], Ana Sovic [2]

Faculty of Electrical Engineering and Computing,University of Zagreb
Unska 3, Zagreb, Croatia
[1] damir.sersic@fer.hr
[2] ana.sovic@fer.hr

Abstract—**In this paper, the relative intersection of confidence intervals (ICI) rule is used to adaptively determine window sizes around each observed point in purpose of denoising. The relative ICI rule defines neighbourhoods of similar statistical properties for every signal sample. If we calculate a mean value on each window, it corresponds to the zero-order estimation and results in a denoised signal. Furthermore, the mean value can be replaced by median for additional robustness of estimation. The same approach could be taken on images. In this paper, we find the maximum window length in four, eight or sixteen directions around each pixel. Mean or median value of chosen surrounding pixels results in a denoised estimation of each observed pixel. The proposed denoising method was tested on an example of a piece-wise constant image and compared to known methods. Under the given conditions, it has shown improvement in terms of the PSNR, MAE and subjective visual impression.**

Keywords: Intersection of confidence intervals, image denoising, mean, median, adaptive filters

I. INTRODUCTION

An image is often corrupted by noise due to imperfectness of sensors or due to transmission. Hence, image denoising is an important issue in many areas, especially in medicine [1], astronomy [2], microscopy [3], object detection, photo restoration, visual tracking and image segmentation.

The goal of denoising is to remove the noise while retaining as much as possible of the important signal features. If an image has a local polynomial structure and contains some additive noise, wavelet based denoising methods are a good approach [4][5][6]. They work fine, except for the edges, where annoying ringing effects are usually present. To avoid ringing and to achieve better results, adaptive methods were introduced, such as shape adaptive DCT [7], block-matching and 3D filtering algorithm [8] or several methods based on the relative intersection on confidence intervals rule (RICI) [9][10][11].

In this paper we propose four, eight or sixteen directions mean and median based RICI algorithm around every pixel to denoise a class of piece-wise constant images.

II. INTERSECTION OF CONFIDENCE INTERVALS

Input signal $x(n)$ is corrupted by additive zero mean Gaussian noise $w(n)$, $\mathcal{N}(0, \sigma_w^2)$:

$$y(n) = x(n) + w(n). \tag{1}$$

Our goal is to find a quite simple and efficient zero-order estimate $\bar{x}(n)$ of the input signal that preserves edges and accurately restores smooth regions. We use moving average estimate with short window near edges and long window in the middle of the regions. We use intersection of confidence intervals (ICI) rule to decide on window lengths [12].

Confidence interval $D_k(n) = [L_k(n), U_k(n)]$ is defined by its interval limits

$$\begin{aligned} L_k(n) &= \bar{x}_{h_k}(n) - \Gamma \cdot \sigma_{h_k}(n), \\ U_k(n) &= \bar{x}_{h_k}(n) + \Gamma \cdot \sigma_{h_k}(n), \end{aligned} \tag{2}$$

where h_k is window length, threshold parameter Γ defines the confidence interval width and $\sigma_{h_k}(n) = \sigma_w/\sqrt{h_k}$ is the deviation of the signal sample estimate. The smallest upper and the largest lower limits on observed interval we denote as:

$$\begin{aligned} \overline{L}_k(n) &= \max_{i=1,\dots,k} L_i(n), \\ \underline{U}_k(n) &= \min_{i=1,\dots,k} U_i(n). \end{aligned} \tag{3}$$

We increase h_k until we reach the largest window length h^+ for which the ICI condition

$$\overline{L}_k(n) \le \underline{U}_k(n) \tag{4}$$

is satisfied.

The window length depends on parameter Γ and is usually slightly too long: a few samples with different statistical properties enter the window to activate the stop criterion. Hence, we apply the RICI rule. If r_c is a preset threshold parameter, then the chosen window length is the largest $h^+ = h_k$ for which is still satisfied:

$$\frac{\underline{U}_k(n) - \overline{L}_k(n)}{U_k(n) - L_k(n)} \ge r_c. \tag{5}$$

The RICI rule is applied as an additional criterion to the ICI rule and gives more accurate estimates $\bar{x}_{h^+}(n)$ for every sample of $y(n)$ [13][14].

III. Image denoising algorithm

A noisy image $y(n,m)$ consists of input image $x(n,m)$ and additive zero-mean Gaussian noise $w(n,m)$, $\mathcal{N}(0,\sigma_w^2)$:

$$y(n,m) = x(n,m) + w(n,m). \tag{6}$$

We propose a directional image denoising method with an arbitrary number of directions. We find optimal window lengths using the ICI or RICI rule in every direction. Then, we calculate an average value of all involved pixels around every observed pixel. The result is a good estimation of the original noiseless input image.

We diversify three special cases of denoising methods: four directions, eight directions and 16 directions. All proposed methods are presented in the sequel.

A. Four directions mean and median RICI

For each image pixel, we observe its row and column (Figure 1a). We apply the ICI / RICI algorithm to the left and to the right in horizontal direction, and up and down in vertical direction. We get four window lengths: h_l^+, h_r^+, h_u^+ and h_d^+, respectively. They determine a cross-like structure with non-even rays. Considering all the included pixels, we calculate an average estimate of the observed pixel $y(n,m)$:

$$\begin{aligned} y_{row}(n,m) = \{&y(n, m - h_r^+(n,m) + 1),\\ &y(n, m - h_r^+(n,m) + 2), \dots,\\ &y(n,m), \dots,\\ &y(n, m + h_l^+(n,m) - 2),\\ &y(n, m + h_l^+(n,m) - 1)\}, \end{aligned} \tag{7}$$

$$\begin{aligned} y_{column}(n,m) = \{&y(n - h_u^+(n,m) + 1, m),\\ &y(n - h_u^+(n,m) + 2, m), \dots,\\ &y(n-1,m), \dots, y(n+1,m)\\ &y(n + h_d^+(n,m) - 2, m),\\ &y(n + h_d^+(n,m) - 1, m)\}. \end{aligned} \tag{8}$$

$$\overline{x_4}(n,m) = \text{mean}\{y_{row}(n,m), y_{column}(n,m)\}. \tag{9}$$

Now we introduce a very weak assumption that the noise is arbitrary but symmetrically distributed. In asymptotical sense ($h^+ \to \infty$), mean can be replaced by median [15]:

$$\overline{x_{4m}}(n,m) = \text{median}\{y_{row}(n,m), y_{column}(n,m)\}. \tag{10}$$

Previously introduced Gaussian noise satisfies the assumption, too. The replacement results in more robustness: proposed method works fine even if the four window lengths were not perfectly determined. It has been shown that the proposed median based method gives more accurate results for almost any noise distribution, and is significantly less sensitive to choice of parameters Γ and r_c [15]. Consequently, the mean absolute error (MAE) of the proposed method is lower than of the mean based ICI or of the other competing denoising methods.

B. Eight directions mean and median RICI

For each image pixel, we observe its row, column, principal and minor diagonal (Figure 1b) to get more pixels for calculating the estimate value. We apply the ICI / RICI rule to the left and to the right along the row, up and down along the column, up-left and down-right along the principal diagonal and up-right and down-left along the minor diagonal. It corresponds to an 8-ray star-like structure. We get eight window lengths: h_l^+, h_r^+, h_u^+, h_d^+, h_{ul}^+, h_{dr}^+, h_{ur}^+ and h_{dl}^+. Considering all the involved pixels, we estimate each observed pixel $y(n, m)$ using mean and median:

$$\begin{aligned} y_{pd}(n,m) = \{&y(n - h_{ul}^+(n,m) + 1,\\ &\quad m - h_{ul}^+(n,m) + 1), \dots\\ &y(n - h_{ul}^+(n,m) + 2, m - h_{ul}^+(n,m) + 2),\\ &y(n-1, m-1), y(n+1, m+1), \dots\\ &y(n + h_{dr}^+(n,m) - 1, m + h_{dr}^+(n,m) - 1)\}, \end{aligned} \tag{11}$$

$$\begin{aligned} y_{md}(n,m) = \{&y(n - h_{ur}^+(n,m) + 1,\\ &\quad m + h_{ur}^+(n,m) - 1), \dots\\ &y(n - h_{ur}^+(n,m) + 2, m + h_{ur}^+(n,m) - 2),\\ &y(n-1, m+1), y(n+1, m-1), \dots\\ &y(n + h_{dl}^+(n,m) - 1, m - h_{dl}^+(n,m) + 1)\}, \end{aligned} \tag{12}$$

$$\begin{aligned} \overline{x_8}(n,m) = \text{mean}\{&y_{row}(n,m), y_{column}(n,m),\\ &y_{pd}(n,m), y_{md}(n,m)\}. \end{aligned} \tag{13}$$

$$\begin{aligned} \overline{x_{8m}}(n,m) = \text{median}\{&y_{row}(n,m), y_{column}(n,m),\\ &y_{pd}(n,m), y_{md}(n,m)\}. \end{aligned} \tag{14}$$

C. Sixteen directions mean and median RICI

To get even more pixels for calculating estimated value of the pixel (n,m), we added extra eight directions – one by one between row, column, principal and minor diagonal (Figure 1c). We found their window lengths using the ICI / RICI rule and applied mean or median to all included pixels in the same way as previously described. Estimated values are denoted as $\overline{x_{16}}(n,m)$ and $\overline{x_{16m}}(n,m)$.

IV. Simulation results

We created an 64x64 artificial image that depicts a dark gray apple on a light gray background (Figure 2a). We added zero mean Gaussian noise $\sigma_w = 20$ (Figure 2b). The image is denoised using undecimated Haar wavelets with hard threshold set to $3.5\sigma_w$ and four decomposition levels (Figure 2c). Big gray areas at the background are good denoised, but there are problems near the edges: ringing effects. Figure 2d shows denoising using Portilla method [4]. Background is not smooth enough, and the edges are not sharp. Anisotropic LPA

– ICI method $\Gamma = 1.05$ is shown in the Figure 2e [10]. We can still see many gray pixels on the background instead of the unique color. The result of separable image denoising based on the RICI rule using fixed weights ($\Gamma = 4.4$ and $r_c = 0.85$) is shown in Figure 2f [9]. Pixel estimates are calculated from pixels in its row and column, separately. We can still see resulting disturbed edges.

In the proposed four directions method, we observe rows and columns around each pixel at the same time and calculate their mean or median value (Figure 2g and 2h). The edges are well restored, but there are some checkerboard effects at the background. The effects are less visible and the PSNR is better for the median based method. If we add extra four directions: principal and minor diagonal, we get the results depicted in Figure 2i and 2j. The true gray color from the apple edge is accurately restored, and the background is better (especially in the median case), as more pixels were involved for calculating the estimate values. Finally, we add extra eight directions (Figure 2k and 2l). The best visual results and the best PSNR are gotten using 16-directions median based RICI in Figure 2l. The apple, background and the edges are almost faultlessly restored.

The PSNR-s for 30 different realizations of the zero mean Gaussian noise $\sigma_w = 20$ and of all mentioned denoising methods are compared in Table 1. All directional methods using median have better PSNR-s than the other methods. The best PSNR is achieved by eight directions median based method. Minimum MAE is gotten by sixteen directions median method, but is very close to eight directions results. If we compare computational times for all the methods we can see that the four directions is the fastest one (except for the Haar) and eight directions method is close.

We checked the results for different noise levels. Figure 3 shows PSNR-s for mentioned methods in range of $\sigma_w \in [0,100]$. Separable RICI methods result in better PSNR-s for smaller σ_w, but after $\sigma_w = 20$ they become the worst. Undecimated Haar wavelet and anisotropic LPA-ICI methods show the best results for high levels of noise, but they are the worst for small levels. Eight and 16 directions median based methods show very similar PSNR-s, with the best results in the middle range of $\sigma_w \in [20,30]$. Considering all the facts, as well as the numerical effectiveness of the method and visual quality of the results, we choose eight directions median based RICI method as our number one choice.

Figure 4 shows a comparison of denoising methods applied to test image *Cameraman*. We added extra Gaussian ($\sigma_w = 20$) and salt & peppers noise. Gaussian noise is well suppressed using almost all described methods. The impact of the salt & peppers noise (ringing around the pixels) is the lowest when using 8-direction median RICI method.

TABLE 1. PSNR, MAE AND COMPUTATIONAL TIMES FOR 30 REALIZATIONS OF THE TEST IMAGE *APPLE*. TESTS ARE MADE ON A COMPUTER WITH INTEL CORE2 DUO CPU 2.67 GHZ, AND 2,00 GB OF RAM.

Method	PSNR	MAE	time, s
noisy-image	22.1197	15.9461	-
separable fixed	32.3026	3.8364	2.4818
separable variable	31.9609	3.8692	2.4818
mean 4 directions	33.4788	3.1810	1.1861
median 4 directions	34.0270	3.0390	1.1889
mean 8 directions	33.4195	2.9605	1.9558
median 8 directions	**34.2846**	2.6006	1.9655
mean 16 directions	30.2518	4.8973	8.3111
median 16 directions	34.2490	**2.2421**	8.3449
anisotropic LPA-ICI	33.2576	3.0041	2.4897
Haar wavelet	28.9898	4.3921	**0.0357**
Portilla	29.6749	5.0579	0.1509

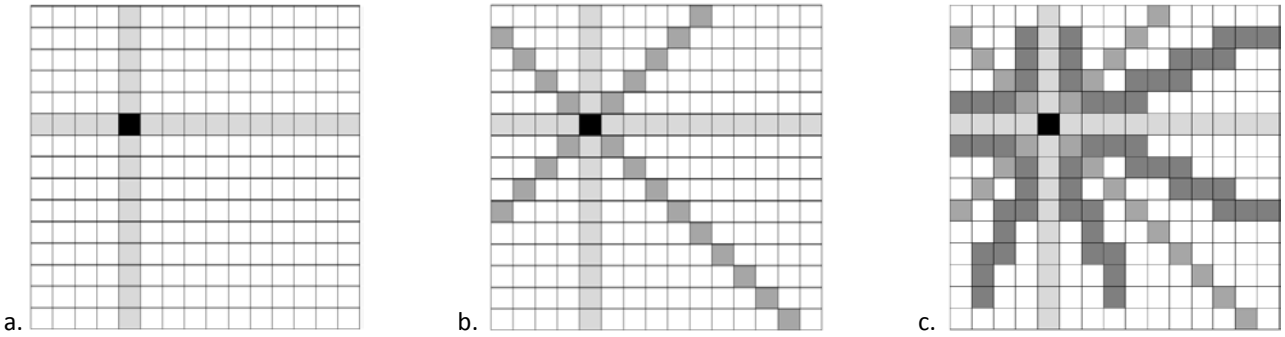

Figure 1. Window directions around the observed black pixel: (a) four, (b) eight and (c) sixteen directions.

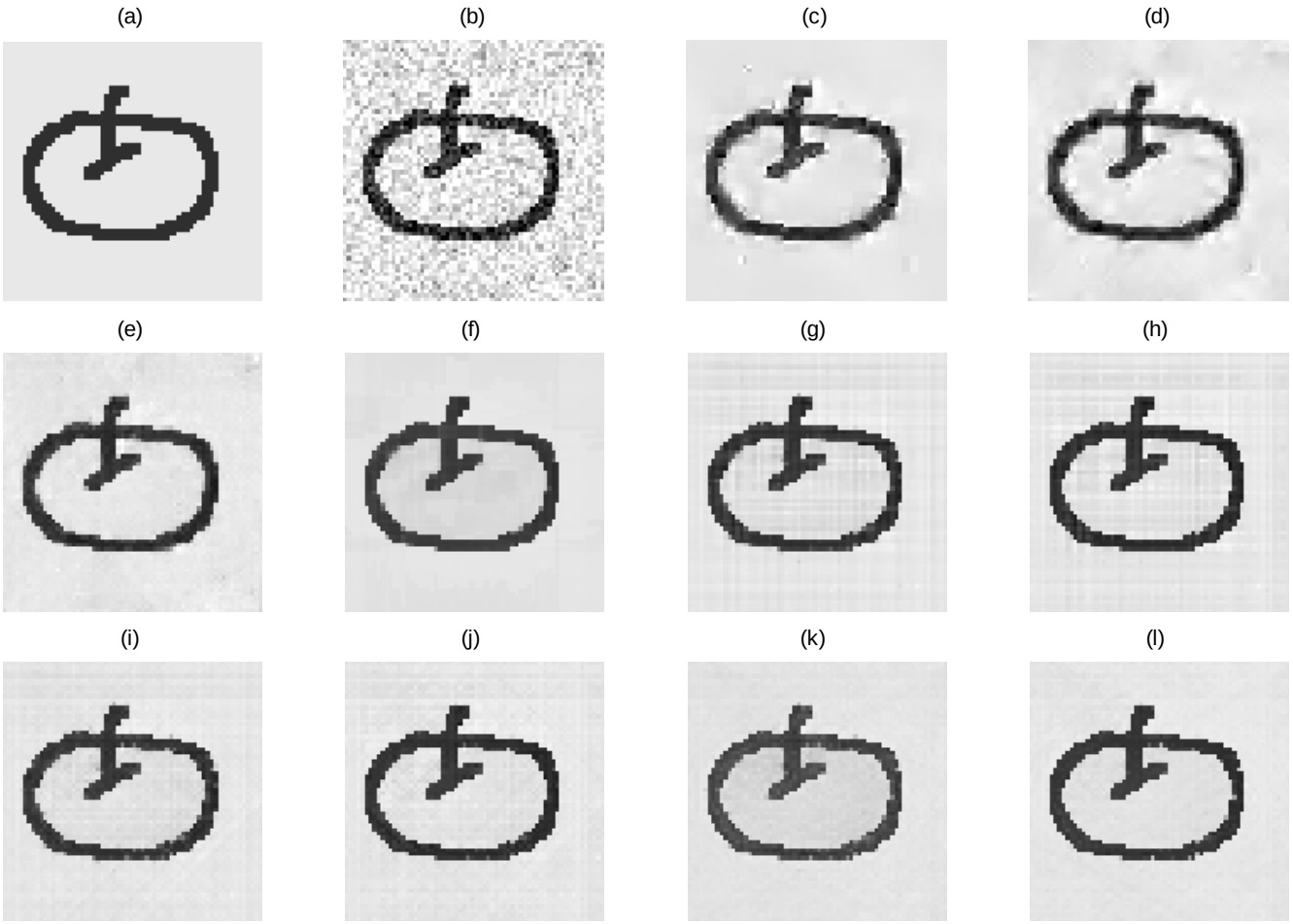

Figure 2. (a) Test noise free image, (b) noisy image with zero mean Gaussian noise $\sigma_w = 20$, (c) undecimated Haar wavelet denoised image with hard threshold $3.5\sigma_w$ and 4 decomposition levels, (d) Portilla method [4], (e) anisotropic LPA-ICI denoised image with $\Gamma = 1.05$, (f) mean RICI ($\Gamma = 4.4, r_c = 0.85$) with fixed weights, (g) four directions mean RICI, (h) four directions median RICI, (i) eight directions mean RICI, (j) eight directions median RICI, (k) 16 – directions mean RICI, (l) 16 – directions median RICI.

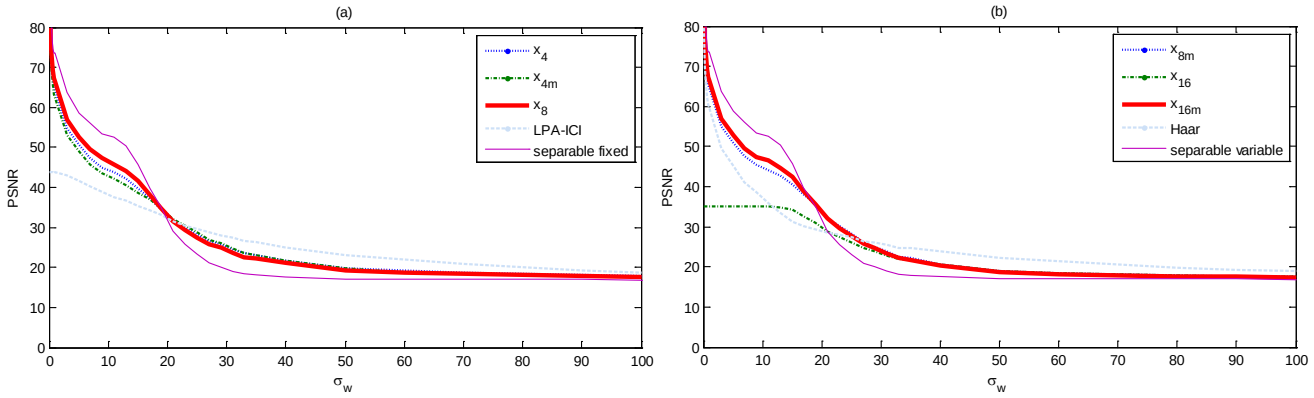

Figure 3. PSNR for the test image with additive zero mean Gaussian noise with different deviations σ_w. The image is denoised using: (a) four directions mean and median, eight directions mean, anisotropic LPA-ICI and separable mean RICI with fixed weights, (b) eight directions median, sixteen directions mean and median, undecimated Haar wavelet and separable mean RICI with variable weights.

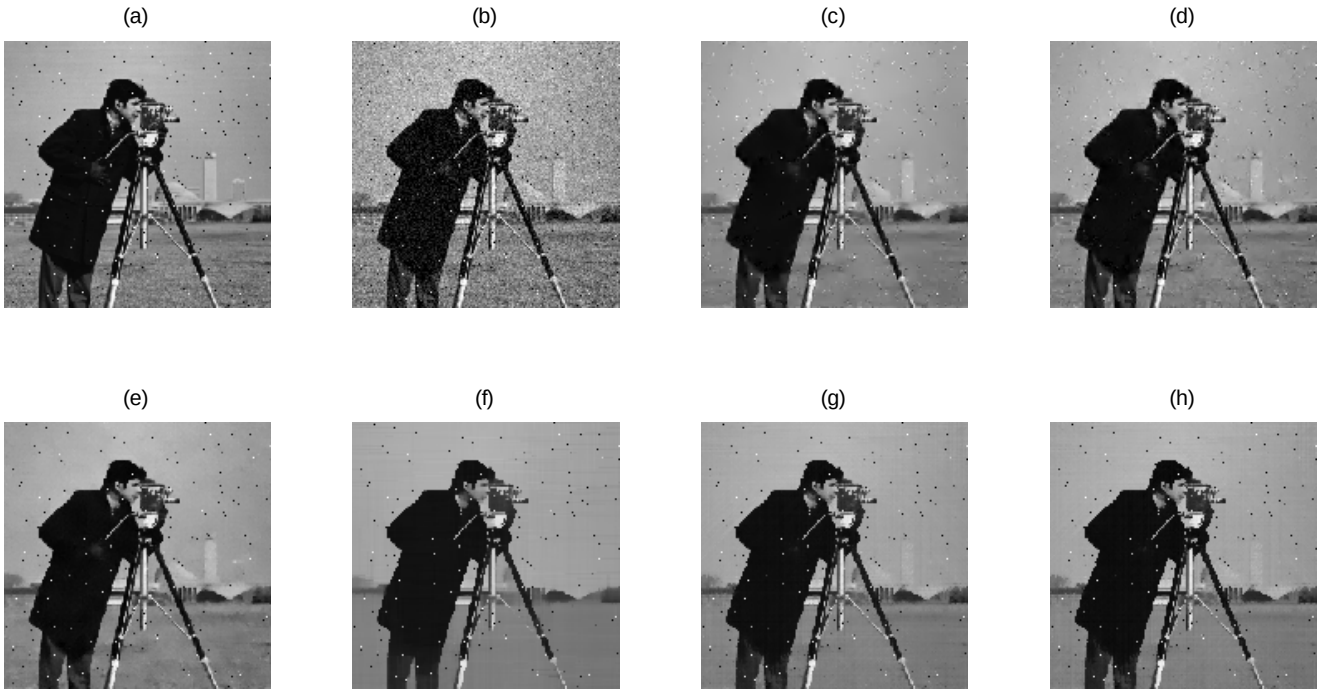

Figure 4. (a) Test mage *Cameraman* with salt&peppers noise, (b) noisy image with zero mean Gaussian noise $\sigma_w = 20$, (c) undecimated Haar wavelet denoised image with hard threshold $3.5\sigma_w$ and 4 decomposition levels, (d) Portilla method [4], (e) anisotropic LPA-ICI denoised image with $\Gamma = 1.05$, (f) mean RICI ($\Gamma = 4.4, r_c = 0.85$) with fixed weights, (g) eight directions mean RICI, (h) eight directions median RICI.

V. Conclusion

In this paper, we proposed novel methods for image denoising that are based on the relative intersection of confidence interval rule. They consider four, eight or sixteen directions around each pixel for calculating estimated value of denoised image. Moreover, they use mean or median based estimators. After comparison of the obtained PSNR-s, MAE-s, visual results and computational times on the test image, we chose eight directions median method as an optimal denoising method for a class of the piece-wise constant images with strong edges.

References

[1] M. Tomic, S. Loncaric, D. Sersic, "Adaptive spatio-temporal denoising of fluoroscopic X-ray sequences", Biomedical Signal Processing and Control, In Press, Corrected Proof, 2011.

[2] R. Puetter, T. Gosnell, and A. Yahil, "Digital image reconstruction: deblurring and denoising," Annual review of astronomy and astrophysics, vol. 43, pp. 139–194, 2005.

[3] G. Cristobaly, M. Chagoyenz, B. Escalante-Ramirezx, and J. R. Lopez, "Wavelet-based denoising methods. a comparative study with applications in microscopy," in Proc. SPIE's 1996 International symposium on optical science, engineering and instrumentation, 1996.

[4] J. Portilla, V. Strela, M. Wainwright, and E. P. Simoncelli, "Image denoising using Gaussian scale mixtures in the wavelet domain," IEEE Trans. Image Process. vol. 12, no.11, pp. 1338–1351, 2003.

[5] A. Sović, D. Seršić, "Adaptive wavelet image decomposition using LAD criterion", In Proc. of the Eusipco, Spain, 2011.

[6] M. Vrankić, D. Seršić, "Image denoising based on adaptive quincunx wavelets," In Proc. of the IEEE 6th Workshop on MSP, Omnipress, Italy, pp. 251-254, 2004.

[7] A. Foi, V. Katkovnik, K. Egiazarian, „Pointwise shape-adaptive DCT for high-quality denoising and deblocking of grayscale and color images," IEEE Transactions on Image Processing, 16(5), pp. 1395–1411, 2007.

[8] K. Dabov, A. Foi, V. Katkovnik, K. Egiazarian, „Image denoising by sparse 3d transform-domain collaborative filtering," IEEE Transactions on Image Processing, 16(8), 2080–2095, 2007.

[9] J. Lerga, V. Sučić, M. Vrankić. "Separable Image Denoising Based on the Relative Intersection of Confidence Intervals Rule," Informatica, 22, 3; pp. 383-394, 2011.

[10] A. Foi, V. Katkovnik, K. Egiazarian, J. Astola. "A novel anisotropic local polynomial estimator based on directional multiscale optimizations," Proceedings of the 6th IMA International Conference Mathematics in Signal Processing, Cirencester, U.K., pp. 79–82. 2004.

[11] V. Katkovnik, K. Egiazarian, J. Astola. "Application of the ICI principle to window size adaptive median filtering," Signal Processing, vol. 83, no. 2, pp. 251–257, 2003.

[12] V. Katkovnik, "A new method for varying adaptive bandwidth selection," IEEE Trans. Signal Process., vol. 47, no. 9, pp. 2567–2571, 1999.

[13] J. Lerga, M. Vrankic, V. Sučić, "A Signal Denoising Method Based on the Improved ICI Rule," IEEE Signal Process. Letters, vol. 15, pp. 601-604, 2008.

[14] J. Lerga, V. Sučić, D. Seršić: „Performance Analysis of the LPA-RICI Denoising Method," 6th International Symposium on Image and Signal Processing and Analysis ISPA 2009, Salzburg, Austria, 2009.

[15] D. Seršić, A. Sović: „A robust improvement of the ICI rule for signal denoising," 7th International Symposium on Image and Signal Processing and Analysis ISPA 2011, Dubrovnik, Croatia, 2011.